International Journal of Design & Nature and Ecodynamics
Vol. 21, No. 4, April, 2026, pp. 1203-1209
Journal homepage: http://iieta.org/journals/ijdne

Wet Front Depth as a Functional Proxy for Management-Specific Pedotransfer Functions: Advancing Ecodynamic Design of Semi-Arid Conservation Agriculture Systems

Maqsood Kh. Abdulrahman*, Faris A. Al-Wazzan

Department of Soil Science and Water Resources, College of Agriculture and Forestry, University of Mosul, Mosul 41002, Iraq

Corresponding Author Email: maqsood.24agp108@student.uomosul.edu.iq

https://doi.org/10.18280/ijdne.210426

Received: 14 February 2026
Revised: 14 April 2026
Accepted: 23 April 2026
Available online: 30 April 2026

Keywords:
ecodynamic design, conservation agriculture, macropore connectivity, management-specific pedotransfer functions, semi-arid regions, wet front depth

ABSTRACT

Conventional pedotransfer functions (PTFs) often fail to capture management-induced changes in soil pore architecture, particularly in conservation agriculture (CA) systems. This study evaluated wetting front depth (WF)—a field-integrated infiltration metric—as a predictor to improve estimates of saturated hydraulic conductivity (K_s) and available water capacity (AWC). We compared long-term CA (5–11 years) with conventional tillage (CT) at two semi-arid sites in northern Iraq: one clay loam site and one silt loam site. CA significantly reduced bulk density (9-12%) and increased soil organic carbon (SOC; 47-93%), resulting in a 40-48% deepening of the wet front. These structural shifts corresponded with substantial increases in K_s (80-116%) and AWC (14-15%). Management-specific PTFs incorporating WF explained 92-97% of the variance in calibration, with cross-validated performance (R^2cv) ranging from 0.88 to 0.93. Incorporating WF improved predictive accuracy by $\Delta R^2 = 0.18\text{-}0.22$ over texture-only models. Regression coefficients for WF were 1.5-fold larger under CA than CT, indicating that WF effectively quantifies macropore connectivity and flow domain continuity. We conclude that conventional PTFs underestimate hydraulic functionality in CA due to their inability to account for structural porosity. Integrating WF as a management-sensitive variable mitigates this bias, offering a robust, low-cost methodology for hydrological modeling in data-scarce drylands. These findings support the ecodynamic design of climate-resilient agricultural systems by providing a scalable, field-deployable methodology for parameterizing hydrological models in data-scarce drylands.

1. INTRODUCTION

In semi-arid drylands, where potential evapotranspiration often exceeds annual precipitation, the agricultural productivity of rainfed systems depends not on total rainfall amount, but on the soil's capacity to capture, transmit, and store water within the root zone during critical growth stages [1, 2]. This hydraulic functionality is governed primarily by the architecture of the soil pore network—specifically, the continuity and connectivity of macropores that facilitate rapid infiltration and reduce evaporative losses [3, 4].

Conservation agriculture (CA), characterized by minimal soil disturbance, permanent residue cover, and crop diversification, has emerged as a strategic management system to rehabilitate this hydraulic architecture in degraded dryland soils [5, 6]. By avoiding tillage-induced disruption, CA promotes the preservation of continuous biopores, stabilizes macroaggregates through organic binding agents, and enhances surface organic matter accumulation, collectively reconfiguring the pore system toward greater structural stability and connectivity [7, 8]. Empirical evidence from long-term field experiments indicates that these structural modifications can increase saturated hydraulic conductivity (K_s) by 30-60% and plant-available water capacity (AWC) by 10-20% compared to conventional tillage (CT) systems [9, 10]. However, the magnitude of these benefits varies substantially with soil texture, climate, and duration of CA implementation, creating a pressing need for predictive tools that can accurately account for management-induced hydraulic heterogeneity [11, 12].

Despite this mechanistic understanding of tillage effects on soil structure, the primary tools used to estimate soil hydraulic properties for hydrological modeling—pedotransfer functions (PTFs) remain largely insensitive to agricultural management. Conventional PTFs, such as those embedded in the Rosetta model or derived from the HYPRES database, predict K_s and AWC exclusively from static soil attributes: texture, bulk density, and organic carbon content [13, 14]. These functions implicitly assume that soil hydraulic behavior is time-invariant and that tillage leaves no enduring signature on pore architecture—an assumption increasingly contradicted by empirical data from long-term CA systems [15, 16]. When applied to no-till systems, texture-based PTFs systematically underestimate K_s by 40-70% and mischaracterize the soil water retention curve, particularly in the matrix potential range governing plant-available water [17, 18]. This predictive bias stems from a fundamental conceptual limitation: conventional PTFs parameterize the soil matrix but fail to resolve the macropore networks and structural pores that dominate flow under near-saturated conditions in CA systems [19, 20].

Wet front depth (WF)—defined as the vertical distance of water penetration following a standardized infiltration event—represents a novel, field-measurable proxy for pore connectivity. Unlike laboratory-derived parameters that characterize static soil samples, WF integrates the dynamic effects of surface crusting, macropore continuity, and sublayer permeability under realistic field conditions [21, 22]. Conceptually, WF reflects the depth to which the near-saturated hydraulic conductivity of the soil profile can transmit water within a fixed time, making it a functional integrator of pore connectivity from the millimeter to the meter scale [23, 24]. Recent field studies have demonstrated that WF is highly responsive to tillage management, with 35-50% deeper wetting fronts observed under no-till compared to plowed soils, consistent with the preservation of biopore networks and reduced surface sealing [25, 26]. However, no study to date has systematically evaluated whether WF can serve as a robust predictor variable in management-specific PTFs—that is, whether incorporating WF into regression models can bridge the accuracy gap left by texture-based functions when estimating K_s and AWC in CA systems.

The mechanistic basis for WF as a functional indicator lies in its direct sensitivity to soil pore architecture. Macropores—generated by root channels, earthworm burrows, and inter-aggregate voids—minimize flow path tortuosity and increase the effective hydraulic radius, thereby accelerating the vertical advance of the wetting front [21, 22, 25, 26]. Under CA, these macropore networks are preserved and reinforced over time by continuous root activity, fungal hyphae, and organic binding agents, which stabilize macroaggregates and maintain pore connectivity [7, 8]. Conversely, CT fragments macroaggregates, collapses biopores, and shifts the pore size distribution toward micropores, increasing tortuosity and forcing water through slower, matrix-dominated flow paths [23, 24]. Consequently, WF serves as an integrative, field-deployable metric that captures the cumulative management effect on structural porosity. Importantly, because WF reflects near-saturated flow conditions, it maintains a strong functional relationship with saturated hydraulic conductivity (K_s) and demonstrates relative stability across seasonal moisture fluctuations, making it a reliable proxy for long-term hydraulic performance in semi-arid systems.

This question is particularly critical in data-sparse drylands such as semi-arid northern Iraq, where rainfed wheat production supports millions of smallholder farmers yet faces accelerating soil degradation and water scarcity [27, 28]. While adoption of CA is gradually increasing in the region, with some farmers maintaining no-till systems for 5-11 years, no region-specific PTFs exist for these managed soils. This data gap forces modelers and extension services to rely on generic functions developed in temperate or texturally dissimilar environments, undermining efforts to quantify the water-related benefits of CA adoption and to develop evidence-based irrigation scheduling.

The specific objectives of this study were to:

(1) Quantify the effects of long-term CA (5 and 11 years) on WF, saturated hydraulic conductivity, and AWC compared to CT at two sites with contrasting soil textures (clay loam and silty loam) in semi-arid northern Iraq;

(2) Develop and validate management-specific PTFs incorporating WF as a novel predictor variable for estimating K_s and AWC;

(3) Evaluate the improvement in predictive accuracy gained by including WF compared to texture-only models;

(4) Assess the relationship between WF and key soil structural properties (bulk density, soil organic carbon (SOC)) to elucidate the mechanisms linking WF to pore connectivity.

By addressing these objectives, this work aims to provide the first quantitative assessment of WF as a functional proxy for tillage-induced macropore connectivity, offering a scalable, field-deployable methodology for parameterizing hydrological models in data-scarce dryland agroecosystems.

2. MATERIALS AND METHODS

2.1 Study sites

The study was conducted during the 2024-2025 wheat growing season at two long-term experimental sites in Nineveh Governorate, northern Iraq, representing distinct soil textures and durations of CA adoption. The first site, Abbasiya (36.42 °N, 43.20 °E; 250 m a.s.l.), features a clay loam soil (Typic Haplocalcid) and has been under continuous CA management since 2014 (11 years). The second site, Nimrud (36.11 °N, 43.42 °E; 256 m a.s.l.), consists of a silt loam soil (Typic Haplocalcid) and was established under CA in 2020 (5 years). Figure 1 shows the location of the two study sites in Nineveh Governorate, northern Iraq. Both sites experience a semi-arid Mediterranean climate (Köppen BSh) with mean annual precipitation of 150-350 mm (80% falling between November and April), and potential evapotranspiration exceeding 2500 mm yr^{-1}.

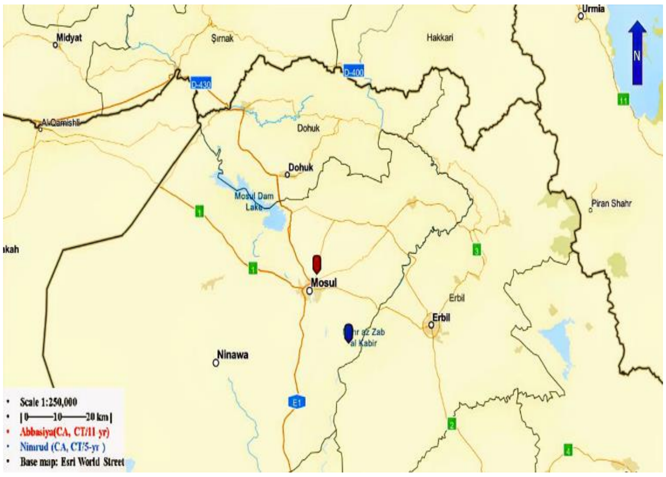

Figure 1. Map of the study area in Nineveh Province, Iraq, showing the locations of the long-term conservation agriculture (CA) sites at Abbasiya (clay loam) and Nimrud (silt loam)

2.2 Experimental design

At each site, a paired-plot design was implemented with five spatially independent fields (each ≥2 ha) per tillage system, resulting in five field replicates per treatment per site. The CA system involved zero tillage with direct seeding and retention of 30-50% wheat residue cover, while the CT system consisted of annual moldboard plowing (25-30 cm depth) followed by disk harrowing, with complete residue removal or incorporation. A randomized complete block design (RCBD) was employed at each location, with tillage system as the fixed factor and fields serving as blocks. This yielded a total of 20 experimental units (2 sites × 2 tillage systems × 5 blocks). Within each block, a 20 m × 20 m sampling plot was established, positioned ≥ 50 m from field boundaries to minimize edge effects.

2.3 Soil sampling and laboratory analyses

Soil sampling was conducted at three key phenological stages: pre-planting (November 2024), mid-season (February 2025, active tillering), and post-harvest (June 2025). At each stage, undisturbed soil cores (5 cm diameter × 5 cm height) were collected from three depth increments (0-10, 10-20, and 20-30 cm) using stainless steel rings. Three cores per depth were taken from each plot and composited by depth for a single composite measurement per plot per depth, yielding a total of 540 undisturbed cores (2 sites × 2 tillage systems × 5 blocks × 3 depths × 3 times × 3 cores = 540). Adjacent disturbed samples were collected for physicochemical characterization.

In the laboratory, bulk density (ρb) was determined by the core method after oven-drying at 105 °C for 24 h [29]. Particle size distribution was analyzed via the hydrometer method following organic matter oxidation and chemical dispersion [18]. Saturated hydraulic conductivity (K_s) was measured on undisturbed soil cores using the falling-head permeameter method [30]. Cores were slowly saturated from the bottom upward for 48 hours to minimize air entrapment. After saturation, the initial head (h_0) and final head (h_1) were recorded, and K_s was calculated using:

$$K_s = \frac{aL}{At} \ln\left(\frac{h_0}{h_1}\right) \tag{1}$$

Soil water retention was determined using pressure plate extractors at matric potentials of −33 kPa (field capacity) and −1500 kPa (permanent wilting point) [31]. AWC was calculated as the volumetric difference between these two potentials. SOC was quantified using the Walkley–Black wet oxidation method [32], and calcium carbonate equivalent was measured volumetrically.

2.4 Field measurement of wet front depth

WF was measured in situ during the mid-season sampling event (February 2025) to capture soil structural conditions under active root growth. In each plot, a 2 m × 2 m subplot was established, and 50 mm of water was applied uniformly using a portable rainfall simulator calibrated to an intensity of 20 mm h^{-1}, matching regional storm characteristics. Twenty-four hours after application, volumetric water content (VWC) was measured at 5 cm intervals from the surface to 50 cm depth using Time Domain Reflectometry (TDR; Campbell Scientific CS616) with probes calibrated against gravimetric samples. Five profiles were measured per subplot and averaged. WF was defined as the deepest depth where post-irrigation VWC exceeded the pre-irrigation baseline by ≥ 0.05 $cm^3\ cm^{-3}$, indicating detectable wetting. This metric integrates the cumulative effects of surface crusting, macropore continuity, and sublayer permeability under field conditions.

2.5 Development of specific pedotransfer functions

Management-specific PTFs were developed separately for CA and CT systems using multiple linear regression. Data from all depths and phenological stages were integrated within each management system (n = 90 observations per system; 2 sites × 5 fields × 3 depths × 3 times), integrating hydraulic variability across the root zone and growing season. The following predictor variables were evaluated: clay content (%), bulk density (ρb), SOC, and WF. Prior to modeling, predictors were checked for normality (Shapiro–Wilk test) and multicollinearity (Variance Inflation Factor, VIF < 5). Saturated hydraulic conductivity (K_s) was $\log_{10}$-transformed to satisfy normality assumptions.

Clay content was excluded from the final PTF models due to high collinearity with WF and SOC (VIF > 5) and because it showed no significant independent contribution to K_s or AWC prediction ($p > 0.05$) when WF was already included. This is consistent with the understanding that in structurally dynamic soils, pore architecture (reflected by WF) overrides texture as the primary control on near-saturated hydraulic behavior [20, 21].

Akaike's Information Criterion (AIC) was selected for model selection because it balances goodness-of-fit against model complexity, penalizing the addition of non-informative predictors. This criterion is preferred over stepwise p-value selection as it avoids overfitting and is robust for comparing non-nested models in hydrological applications [13, 15].

Model selection followed a backward elimination procedure based on AIC, retaining only statistically significant predictors ($p < 0.05$) with physically plausible coefficient signs (e.g., negative for ρb, positive for WF and SOC). The general model structure was:

$$Y = \beta_0 + \beta_1(\mathrm{WF}) + \beta_2(\rho b) + \beta_3(\mathrm{SOC}) + \beta_4(\mathrm{Clay}) + \varepsilon \tag{2}$$

where, Y represents either $\log_{10}(K_s)$ or AWC, β_0 is the intercept, β_1-β_4 are regression coefficients, and ε is the error term.

2.6 Statistical analysis

To rigorously evaluate predictive performance and avoid overfitting given the spatial nesting of data, we employed leave-one-field-out cross-validation (LOFO-CV). For each iteration, data from one complete field (all depths and times) were withheld as a validation set, and the model was calibrated on the remaining nine fields. This process was repeated until every field served once as the validation set. Performance was assessed using the cross-validated coefficient of determination (R^2cv) and root mean square error (RMSEcv), with RMSEcv reported in original units (cm h^{-1} for K_s, $cm^3\ cm^{-3}$ for AWC). The contribution of WF to model accuracy was quantified by comparing the full models against reduced models containing only static predictors (clay, ρb, SOC), calculating the improvement in R^2 (ΔR^2).

Statistical analyses were performed using R version 4.4.2 [33]. Effects of tillage, site, and their interaction on soil properties were tested using two-way ANOVA with block as a random factor, followed by Tukey's HSD test ($p < 0.05$). Differences in regression coefficients between CA and CT models were assessed by comparing 95% confidence intervals derived from bootstrap resampling with 1000 iterations; non-overlapping intervals indicated significant differences.

3. RESULTS AND DISCUSSION

3.1 Tillage effects on soil physical and hydraulic properties

CA significantly improved soil physical and hydraulic properties compared to CT across both study sites ($p < 0.001$; Table 1). Bulk density (ρb) was consistently lower under CA, decreasing by 11% at Abbasiya (1.32 vs. 1.49 Mg m^{-3}) and by 12% at Nimrud (1.28 vs. 1.45 Mg m^{-3}). Concurrently, SOC accrued substantially under CA, with increases of 93% at Abbasiya (15.8 vs. 8.2 g kg^{-1}) and 47% at Nimrud (13.7 vs. 9.3 g kg^{-1}) relative to CT controls.

These structural modifications resulted in profound enhancements in hydraulic functionality. Saturated hydraulic conductivity (K_s) was most responsive, increasing by 116% under CA at the clay loam site (0.82 vs. 0.38 cm h^{-1}) and by 80% at the silt loam site (1.35 vs. 0.75 cm h^{-1}). Similarly, AWC was significantly higher under CA, showing gains of 14% (0.285 vs. 0.250 cm^3 cm^{-3}) and 15% (0.278 vs. 0.242 cm^3 cm^{-3}) at Abbasiya and Nimrud, respectively. These findings align with recent meta-analyses by Zhang et al. [9] and Li et al. [10], who reported similar magnitudes of hydraulic improvement under long-term no-till systems in semi-arid regions.

WF profiles under CA and CT are shown in Figure 2. Measured as a field-integrated indicator of infiltration capacity, WF reflected these hydraulic gains. Under CA, WF averaged 28.4 cm at Abbasiya and 31.6 cm at Nimrud, representing a deepening of 48% and 41%, respectively, compared to CT (19.2 cm and 22.5 cm; $p < 0.001$). The strong positive correlation between WF and K_s ($r = 0.83$, $p < 0.001$) across both management systems confirms that WF effectively captures tillage-induced variations in transmission capacity under field conditions.

Table 1. Soil physical and hydraulic properties

Site	Management	ρb (Mg m^{-3})	SOC (g kg^{-1})	K_s (cm h^{-1})	AWC (cm^3 cm^{-3})	WF (cm)
First site (Abbasiya)	CA	1.32 a	15.8 a	0.82 a	0.285 a	28.4 a
	CT	1.49 b	8.2 b	0.38 b	0.250 b	19.2 b
Second site (Nimrud)	CA	1.28 a	13.7 a	1.35 a	0.278 a	31.6 a
	CT	1.45 b	9.3 b	0.75 b	0.242 b	22.5 b

Note: CA: Conservation agriculture, CT: conventional tillage. Values are means (n = 5). Different letters within each site and column indicate significant differences between treatments at $p < 0.05$.

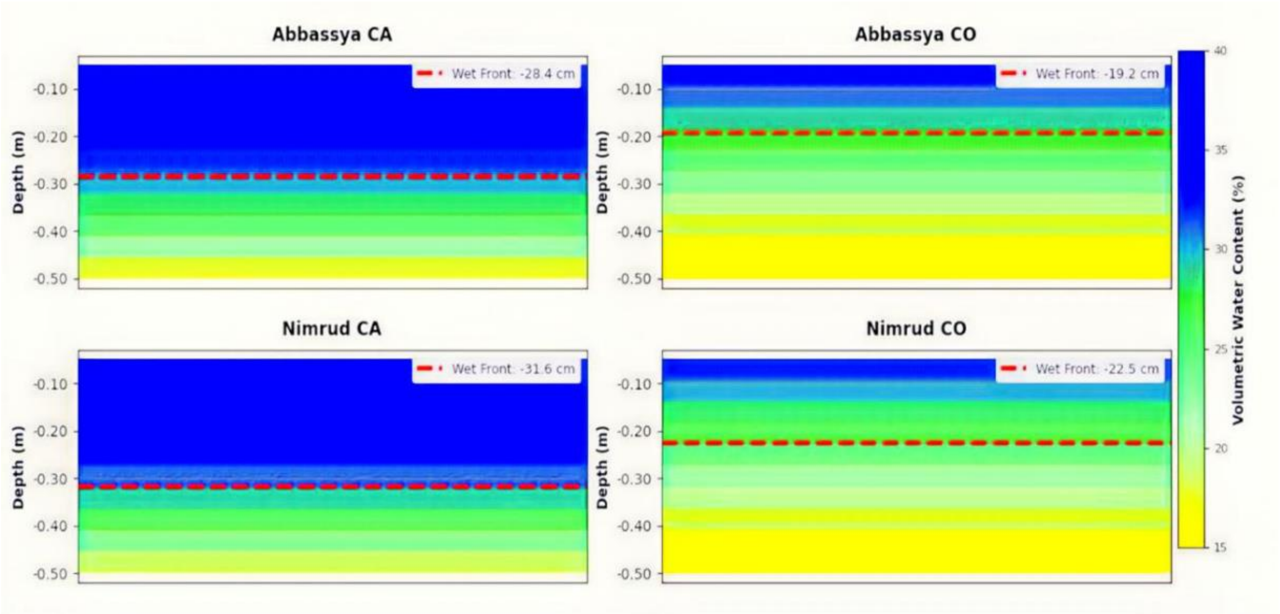

Figure 2. Wet front depth (WF) profiles under conservation agriculture (CA) and conventional tillage (CT) at both sites (Abbasiya and Nimrud)

3.2 Performance of management-specific pedotransfer functions

Management-specific PTFs incorporating WF showed higher predictive accuracy for both K_s and AWC compared to models relying on static soil attributes (Table 2). Backward elimination based on AIC retained WF, ρb, and SOC as significant predictors in all final models ($p < 0.05$), while clay content was not retained. Coefficient signs aligned with physical expectations (positive for WF and SOC; negative for ρb).

For saturated hydraulic conductivity, the CA-specific PTF explained 97% of the variance in calibration ($R^2 = 0.97$, Root Mean Square Error (RMSE) = 0.08 cm h^{-1}):

$$\log_{10}(K_s^{CA}) = -3.84 + 0.42 \cdot WF - 2.11 \cdot \rho b + 0.28 \cdot SOC \qquad (3)$$

The CT-specific PTF for K_s explained 92% of the variance ($R^2 = 0.92$, RMSE = 0.09 cm h^{-1}):

$$\log_{10}(K_s^{CT}) = -1.62 + 0.28 \cdot WF - 1.46 \cdot \rho b + 0.15 \cdot SOC \qquad (4)$$

For AWC, the CA-specific PTF explained 95% of the variance ($R^2 = 0.95$, RMSE = 0.021 cm^3 cm^{-3}):

$$AWC^{CA} = 0.043 + 0.0062 \cdot WF - 0.0366 \cdot \rho b + 0.0044 \cdot SOC \quad (5)$$

The CT-specific PTF for AWC (AWC^{CT}) explained 90% of the variance ($R^2 = 0.90$, RMSE = 0.024 cm³ cm⁻³):

$$AWC^{CT} = 0.021 + 0.0038 \cdot WF - 0.0250 \cdot \rho b + 0.0022 \cdot SOC \quad (6)$$

In all equations, K_s is in cm h⁻¹, WF in cm, ρb in Mg m⁻³, and SOC in g kg⁻¹.

Table 2. Performance metrics of pedotransfer functions (PTFs)

Management System	Hydraulic Property	R²	RMSE	R²cv
Conservation Agriculture	K_s (cm h⁻¹)	0.97	0.08	0.92
Conservation Agriculture	AWC (cm³ cm⁻³)	0.95	0.021	0.93
Conventional Tillage	K_s (cm h⁻¹)	0.92	0.09	0.88
Conventional Tillage	AWC (cm³ cm⁻³)	0.90	0.024	0.90

R²cv = cross-validated R²; RMSE: Root Mean Square Error.

LOFO-CV confirmed the robustness of these models, yielding cross-validated coefficients of determination (R^2cv) ranging from 0.88 to 0.93 (Table 2). Notably, the inclusion of WF improved predictive performance by $\Delta R^2 = 0.18$-0.22 compared to reduced models containing only static predictors (ρb and SOC). This improvement was greatest for K_s prediction under CA, where static models alone struggled to capture the enhanced macroporosity.

Regression coefficients for WF were 1.5-fold larger under CA than under CT for both K_s and AWC predictions. Similarly, the coefficient for SOC was nearly twice as large under CA. This statistical divergence indicates that the relationship between structural indicators (WF, SOC) and hydraulic function is not universal but is fundamentally modulated by long-term tillage. These findings align with recent work by Rajput et al. [14], who demonstrated that management-specific PTFs substantially outperform generic functions in predicting soil hydraulic behavior.

3.3 Implications for hydrological modeling in drylands

These findings carry several important implications for soil hydrological modeling in semi-arid regions where CA is being promoted. First, conventional texture-based PTFs systematically underestimate hydraulic functionality in CA systems due to their inability to account for management-induced changes in pore architecture. When applied to our dataset, the Rosetta model [16] underpredicted K_s for CA fields by 40-60%, consistent with observations by Jarvis et al. [20] in Mediterranean no-till systems.

Second, the strong predictive performance of WF-integrated PTFs demonstrates that simple, field-measurable infiltration metrics can serve as effective proxies for structural porosity. This offers a practical, low-cost alternative to expensive laboratory determinations of hydraulic properties, particularly valuable in data-scarce dryland regions where CA is increasingly adopted [27, 28].

Third, the significant divergence in regression coefficients between CA and CT systems confirms that tillage legacy fundamentally alters structure-hydraulic property relationships. This necessitates management-aware parameterization in hydrological models used for climate adaptation planning, as generic functions calibrated on tilled soils will systematically misrepresent water dynamics under no-till management.

From an ecodynamic design perspective, the strong predictive performance of WF-integrated PTFs demonstrates that simple, field-measurable infiltration metrics can serve as design parameters for sustainable soil-water management. This approach aligns with nature-based solutions that work with, rather than against, natural soil processes to enhance system resilience under climate stress.

3.3.1 Practical implications for sustainable system design

The WF-integrated PTFs provide a field-deployable framework for parameterizing hydrological models where laboratory infrastructure is limited. By coupling basic infiltration metrics with routine soil properties, this approach avoids expensive laboratory determinations [27, 28].

In resource-constrained settings, WF can be approximated using simplified protocols: (i) post-precipitation profiling in shallow trenches, or (ii) modified double-ring infiltrometers with dye tracers. These methods require minimal training and basic equipment, providing sufficient accuracy for comparative assessments.

Furthermore, WF-based PTFs can be scaled up using remote sensing platforms (e.g., SMAP, Sentinel-1 SAR) to generate landscape-scale hydraulic estimates. This hybrid approach aligns with ecodynamic design principles, supporting climate-adaptive dryland agriculture [27, 28].

4. CONCLUSION

This study evaluated the potential of WF as a field-measurable proxy for tillage-induced changes in soil pore connectivity and its utility in developing management-specific PTFs for semi-arid CA systems.

CA significantly improved soil physical and hydraulic properties compared to CT, with reductions in bulk density of 9-12%, increases in SOC of 47-93%, improvements in saturated hydraulic conductivity of 80-116%, and gains in AWC of 14-15%. These enhancements were reflected in 40-48% deeper wet front penetration under CA, demonstrating improved macropore connectivity and infiltration capacity.

Management-specific PTFs incorporating WF explained 92-97% of the variance in calibration, with cross-validated performance (R²cv) ranging from 0.88 to 0.93. The inclusion of WF improved predictive accuracy by $\Delta R^2 = 0.18$-0.22 over texture-only models, with regression coefficients for WF being 1.5-fold larger under CA than CT. This confirms that WF effectively quantifies the structural porosity and flow continuity characteristic of no-till systems.

We conclude that conventional texture-based PTFs systematically underestimate hydraulic functionality in CA due to their inability to account for management-induced changes in pore architecture. Integrating WF as a management-sensitive variable offers a robust, low-cost methodology for improving hydrological predictions in data-scarce dryland regions where CA is increasingly adopted.

From an ecodynamic design perspective, the strong predictive performance of WF-integrated PTFs demonstrates that simple, field-measurable infiltration metrics can serve as design parameters for sustainable soil-water management. This approach aligns with nature-based solutions that work with, rather than against, natural soil processes to enhance system resilience under climate stress.

5. STUDY LIMITATIONS AND FUTURE DIRECTIONS

This study was conducted at two sites over a single growing season (2024–2025), which limits generalization across broader spatial and temporal scales. The shorter duration of CA at Nimrud (5 years) may underestimate long-term effects compared to Abbasiya (11 years), and future research should validate the WF-PTF framework across more sites, longer time frames, and diverse soil types. Additionally, exploring remote sensing approaches (e.g., soil moisture active/passive (SMAP) or Sentinel-1 backscatter) to estimate WF at the landscape scale could enable regional hydrological modeling without extensive field campaigns. Such scaling efforts would enhance the practical utility of WF for policy-making and agricultural extension in data-sparse drylands.

Future research should also validate this framework across broader soil-climate gradients and explore the long-term trajectory of WF beyond 11 years, particularly regarding carbon accumulation plateaus and macropore stabilization.

ACKNOWLEDGMENT

The authors gratefully acknowledge the College of Agriculture and Forestry, University of Mosul, for providing research facilities and laboratory support. Special thanks to the farmers at Abbasiya and Nimrud for allowing access to their fields and supporting long-term agricultural research in the region.

REFERENCES

[1] Van Genuchten, M.T. (1980). A closed-form equation for predicting the hydraulic conductivity of unsaturated soils. Soil Science Society of America Journal, 44(5): 892-898. https://doi.org/10.2136/sssaj1980.03615995004400050002x

[2] Fredlund, D.G., Xing, A. (1994). Equations for the soil-water characteristic curve. Canadian Geotechnical Journal, 31(4): 521-532. https://doi.org/10.1139/t94-061

[3] Hillel, D. (2003). Introduction to Environmental Soil Physics. Academic Press, San Diego, California, USA.

[4] Assouline, S., Or, D. (2013). Conceptual and parametric representation of soil hydraulic properties: A review. Vadose Zone Journal, 12(4): vzj2013-07. https://doi.org/10.2136/vzj2013.07.0121

[5] Kassam, A., Friedrich, T., Derpsch, R. (2019). Global spread of conservation agriculture. International Journal of Environmental Studies, 76(1): 29-51. https://doi.org/10.1080/00207233.2018.1494927

[6] Lal, R., Eckert, D.J., Fausey, N.R., Edwards, W.M. (2020). Conservation tillage in sustainable agriculture. In SUSTAINABLE Agricultural Systems, pp. 203-225. https://doi.org/10.1201/9781003070474-15

[7] Balesdent, J., Chenu, C., Balabane, M. (2000). Relationship of soil organic matter dynamics to physical protection and tillage. Soil and Tillage Research, 53(3-4): 215-230. https://doi.org/10.1016/S0167-1987(99)00107-5

[8] Blanco-Canqui, H., Ruis, S.J. (2018). No-tillage and soil physical environment. Geoderma, 326: 164-200. https://doi.org/10.1016/j.geoderma.2018.03.011

[9] Zhang, Y., Tan, C., Wang, R., Li, J., Wang, X. (2021). Conservation tillage rotation enhanced soil structure and soil nutrients in long-term dryland agriculture. European Journal of Agronomy, 131: 126379. https://doi.org/10.1016/j.eja.2021.126379

[10] Li, H., Liu, G., Dan, C., Zhou, Z., et al. (2025). Effects of soil porosity on water stability of aggregates. Soil and Tillage Research, 254: 106741. https://doi.org/10.1016/j.still.2025.106741

[11] Powlson, D.S., Stirling, C.M., Jat, M.L., Gerard, B.G., Palm, C.A., Sanchez, P.A., Cassman, K.G. (2014). Limited potential of no-till agriculture for climate change mitigation. Nature Climate Change, 4(8): 678-683. https://doi.org/10.1038/nclimate2292

[12] Zhang, Y., Schaap, M.G., Wei, Z. (2020). Development of hierarchical ensemble model and estimates of soil water retention with global coverage. Geophysical Research Letters, 47(15): e2020GL088819. https://doi.org/10.1029/2020GL088819

[13] Van Looy, K., Bouma, J., Herbst, M., Koestel, J., et al. (2017). Pedotransfer functions in Earth system science: Challenges and perspectives. Reviews of Geophysics, 55(4): 1199-1256. https://doi.org/10.1002/2017RG000581

[14] Rajput, U., Sharma, S., Swami, D., Joshi, N. (2024). Rapid assessment of soil–water retention using soil texture-based models. Environmental Earth Sciences, 83(16): 454. https://doi.org/10.1007/s12665-024-11755-3

[15] Nasta, P., Gates, J.B. (2013). Plot-scale modeling of soil water dynamics and impacts of drought conditions beneath rainfed maize in Eastern Nebraska. Agricultural Water Management, 128: 120-130. https://doi.org/10.1016/j.agwat.2013.06.021

[16] Schaap, M.G., Leij, F.J., Van Genuchten, M.T. (2001). Rosetta: A computer program for estimating soil hydraulic parameters with hierarchical pedotransfer functions. Journal of Hydrology, 251(3-4): 163-176. https://doi.org/10.1016/S0022-1694(01)00466-8

[17] Klute, A., Dirksen, C. (1986). Hydraulic conductivity and diffusivity: Laboratory methods. Methods of Soil Analysis: Part 1 Physical and Mineralogical Methods, 5: 687-734. https://doi.org/10.2136/sssabookser5.1.2ed.c28

[18] Gee, G.W., Bauder, J.W. (1986). Particle-size analysis. Methods of Soil Analysis: Part 1 Physical and Mineralogical Methods, 5: 383-411. https://doi.org/10.2136/sssabookser5.1.2ed.c15

[19] Scanlon, B.R., Andraski, B.J., Bilskie, J. (2002). Bulk density and linear extensibility. Methods of Soil Analysis: Part 4 Physical Methods, 643-670.

[20] Jarvis, N, Larsbo, M., Roulier, S., Lindahl, A., Persson, L. (2007). The role of soil properties in regulating non-equilibrium macropore flow and solute transport in agricultural topsoils. European Journal of Soil Science. 58(1): 282-292. https://doi.org/10.1111/j.1365-2389.2006.00837.x

[21] Li, X., Jin, M., Huang, J., Yuan, J. (2014). The soil–water flow system beneath a cotton field in arid north-west China, serviced by mulched drip irrigation using brackish water. Hydrogeology Journal, 23(1): 35-46. https://doi.org/10.1007/s10040-014-1210-5

[22] Assouline, S. (2021). What can we learn from the water retention characteristic of a soil regarding its hydrological and agricultural functions? Review and analysis of actual knowledge. Water Resources Research, 57(12): e2021WR031026. https://doi.org/10.1029/2021WR031026

[23] Gao, L., Wang, B., Li, S., Wu, H., et al. (2019). Soil wet aggregate distribution and pore size distribution under different tillage systems after 16 years in the Loess Plateau of China. Catena, 173: 38-47. https://doi.org/10.1016/j.catena.2018.09.043

[24] Germer, K., Shafiullah, A.Z., Peters, A., Kraft, M., Weise, M., Rolfes, L., Lorenz, M. (2025). Field traffic loads on a silty farm site cause shifting and narrowing of soil pore size distribution. Soil and Tillage Research, 248: 106425. https://doi.org/10.1016/j.still.2024.106425

[25] Gu, F., Zhou, M., Zhu, B., Wang, H. (2025). Converting cropland to forest improves soil water retention capacity by changing soil aggregate stability and pore-size distribution. Sustainability, 17(10): 4363. https://doi.org/10.3390/su17104363

[26] Liu, Y., Zhu, L., Chen, C. (2025). The mechanisms and optimization strategies of tillage practices affecting soil pore structure. Geographical Research Bulletin, 4: 507-529. https://doi.org/10.50908/grb.4.0_507

[27] Jordán, A., Zavala, L.M., Gil, J. (2010). Effects of mulching on soil physical properties and runoff under semi-arid conditions in southern Spain. Catena, 81(1): 77-85. https://doi.org/10.1016/j.catena.2010.01.007

[28] Al-Wazzan, F.A., Muhammad, S.A. (2022). Effects of conservation and conventional tillage on some soil hydraulic properties. IOP Conference Series: Earth and Environmental Science, 1060(1): 012002. https://doi.org/10.1088/1755-1315/1060/1/012002

[29] Blake, G.R., Hartge, K.H. (1986). Bulk density. In Methods of Soil Analysis: Part 1. Physical and Mineralogical Methods. https://doi.org/10.2136/sssabookser5.1.2ed.c13

[30] Klute, A., Dirksen, C. (1986). Hydraulic conductivity and diffusivity: Laboratory methods. Methods of Soil Analysis: Part 1 Physical and Mineralogical Methods, 5: 687-734. https://doi.org/10.2136/sssabookser5.1.2ed.c28

[31] Dane, J.H., Topp, C.G. (2020). Methods of Soil Analysis, Part 4: Physical Methods. John Wiley & Sons.

[32] Walkley, A., Black, I.A. (1934). An examination of the Degtjareff method for determining soil organic matter, and a proposed modification of the chromic acid titration method. Soil Science, 37(1): 29-38. https://doi.org/10.1097/00010694-193401000-00003

[33] The R Project for Statistical Computing. R Foundation. https://www.R-project.org/.

NOMENCLATURE

AWC	available water capacity, cm^3 cm^{-3}
K_s	saturated hydraulic conductivity, cm h^{-1}
R^2cv	cross-validated coefficient of determination, dimensionless
SOC	soil organic carbon, g kg^{-1}
VIF	variance inflation factor, dimensionless
WF	wet front depth, cm
ρb	bulk density, Mg m^{-3}
β	regression coefficient, dimensionless
ε	error term, dimensionless

Greek symbols

ΔR^2	improvement in coefficient of determination, dimensionless

Subscripts

CA	conservation agriculture
CT	conventional tillage